Guided wave propagation in $0.67Pb(Mg_{1/3}Nb_{2/3})O_3-0.33PbTiO_3$ single crystal plate poled along $[001]_c$

Chuanwen Chen, Rui Zhang,[a] and Hui Chen
Department of Physics, Harbin Institute of Technology, Harbin, Heilongjiang 150080, China

Wenwu Cao
Department of Physics, Harbin Institute of Technology, Harbin, Heilongjiang 150080, China and Materials Research Institute, The Pennsylvania State University, University Park, Pennsylvania, 16802

(Received 10 July 2007; accepted 1 August 2007; published online 5 September 2007)

Dispersion relations of Lamb waves and shear horizontal (SH) waves propagating in the [100] and [110] directions of $0.67Pb(Mg_{1/3}Nb_{2/3})O_3-0.33PbTiO_3$ piezoelectric single crystal plate poled along $[001]_c$ were calculated. Multiple crossings between symmetric and antisymmetric modes appear due to the moderate anisotropy of these crystals. As frequency increases, the velocities for SH wave modes approach 2.88 and 0.88 mm/μs, respectively, for waves propagating along [100] and [110] directions. These limiting velocities are the corresponding shear velocities of bulk crystals. © *2007 American Institute of Physics*. [DOI: 10.1063/1.2775093]

$(1-x)Pb(Zn_{1/3}Nb_{2/3})O_3-xPbTiO_3$ (PZN-PT) and $(1-x)Pb(Mg_{1/3}Nb_{2/3})O_3-xPbTiO_3$ (PMN-PT) ferroelectric single crystals with composition near the morphotropic phase boundary (MPB) exhibit superior electromechanical properties at room temperature when being poled along the $[001]_c$ cubic direction.[1–4] From fabrication consideration, PMN-PT single crystals near the MPB are more favored in the next generation electromechanical devices, including piezoelectric transducers, actuators, piezoelectric ultrasonic motors, etc.

Some electromechanical devices use guided waves to achieve the conversion between mechanical energy and electrical energy. Such acoustic guided waves propagating in plates can be decoupled into two kinds of waves, namely, shear horizontal (SH) waves and Lamb waves while Lamb waves can be further divided into symmetric and antisymmetric modes. The zeroth-order symmetric mode (S_0) and antisymmetric mode (A_0) Lamb waves are the most useful ones.[5]

In order to get useful modes or filter out the spurious ones, it is important to know the Lamb wave propagation properties in a specific crystal. Lamb waves have been extensively studied for many years because of their wide applications in nondestructive inspection, material characterization, biosensors, mechanical sensors, and electronic devices.[6–10] Partial wave theory is the most commonly used method for analyzing harmonic wave propagation in anisotropic materials.[11–13]

In this letter, guided wave propagation in $[001]_c$ poled $0.67Pb(Mg_{1/3}Nb_{2/3})O_3-0.33PbTiO_3$ (PMN-0.33PT) single crystal plate is studied by employing the partial wave method. The dispersion relations of Lamb waves and SH waves propagating along the [100] and [110] directions are calculated, which can provide useful information for designing guide wave electromechanical devices using PMN-PT single crystals.

The PMN-0.33PT single crystal is in the ferroelectric phase at room temperature with rhombohedral $3m$ symmetry. When being poled along $[001]_c$ direction, it has a $4mm$ macroscopic symmetry,[14] which has six independent elastic coefficients, three piezoelectric coefficients, and two dielectric coefficients. All material coefficients are available in the literature.[15] The coordinate system used in this work is shown in Fig. 1.

The elastic wave equations in a piezoelectric medium can be written as

$$\rho\frac{\partial^2 u_j}{\partial t^2}-c_{ijkl}\frac{\partial^2 u_k}{\partial x_i\partial x_l}-e_{kij}\frac{\partial^2\phi}{\partial x_i\partial x_k}=0, \tag{1a}$$

$$e_{ikl}\frac{\partial^2 u_k}{\partial x_i\partial x_l}-\varepsilon_{ik}\frac{\partial^2\phi}{\partial x_i\partial x_k}=0 \quad (i,j,k,l,=1,2,3). \tag{1b}$$

Here ρ is the density of the medium, c_{ijkl} are the components of the elastic stiffness tensor at constant electric field, e_{kij} are the components of piezoelectric constant tensor at constant strain, and ε_{ik} are the components of dielectric permittivity tensor at constant strain.

The particle displacements and the potential can be written as linear combinations of partial waves,

$$u_j=\alpha_j\exp(ikbx_3)\exp[ik(x_1-vt)], \tag{2a}$$

$$\phi=\alpha_4\exp(ikbx_3)\exp[ik(x_1-vt)], \tag{2b}$$

where v is the phase velocity of the acoustic wave, k is the magnitude of wave vector $\mathbf{k}$, and b is the decay coefficient of displacement and potential to be determined.

Substituting Eq. (2) into Eq. (1) gives the following equations:

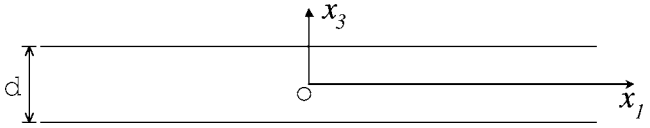

FIG. 1. Coordinate system used in this work.

[a]Electronic mail: ruizhang_ccmst@hit.edu.cn

$$\begin{pmatrix} \Gamma_{11}-\rho v^2 & 0 & \Gamma_{13} & \Gamma_{14} \\ 0 & \Gamma_{22}-\rho v^2 & 0 & 0 \\ \Gamma_{13} & 0 & \Gamma_{33}-\rho v^2 & \Gamma_{34} \\ \Gamma_{14} & 0 & \Gamma_{34} & \Gamma_{44} \end{pmatrix} \begin{pmatrix} \alpha_1 \\ \alpha_2 \\ \alpha_3 \\ \alpha_4 \end{pmatrix} = 0, \tag{3}$$

where $\Gamma_{11}=c_{44}b^2+c_{11}$, $\Gamma_{22}=c_{44}b^2+c_{66}$, $\Gamma_{33}=c_{33}b^2+c_{44}$, $\Gamma_{44}=-(\varepsilon_{33}b^2+\varepsilon_{11})$, $\Gamma_{13}=(c_{13}+c_{55})b$, $\Gamma_{14}=(e_{15}+e_{31})b$, and $\Gamma_{34}=e_{33}b^2+e_{15}$.

In order to have nontrivial solutions, the determinant of the square matrix in Eq. (3) must be set to zero,

$$|\Gamma_{rs}-\delta'_{rs}\rho v^2|=0 \quad (r,s=1,2,3,4,\ \delta'_{44}=0). \tag{4}$$

From Eq. (4) there are eight b values for a fixed v value. Each b value gives the depth dependence of each wave component in a piezoelectric media. For a finite plate, all eight values should be retained, i.e.,

$$u_j=\left\{\sum_n C_n\alpha_j^{(n)}\exp(ikb^{(n)}x_3)\right\}\exp[ik(x_1-vt)],$$
$$n=1{:}8, \tag{5a}$$

$$\phi=\left\{\sum_n C_n\alpha_4^{(n)}\exp(ikb^{(n)}x_3)\right\}\exp[ik(x_1-vt)], \quad n=1{:}8. \tag{5b}$$

Since the surface is assumed to be stress free, the three traction components of stress must vanish on both surfaces. For the short circuit case, the electrical potential ϕ in Eq. (5b) is set to zero at both plate surfaces ($x=\pm d/2$). Thus, the eight boundary conditions for this free plate are

$$T_{31}=0, \tag{6a}$$

$$T_{32}=0, \tag{6b}$$

$$T_{33}=0, \tag{6c}$$

$$\phi=0, \tag{6d}$$

at $x=\pm d/2$. The traction stresses are given by

$$T_{3j}=c_{3jkl}(\partial u_k/\partial x_l)+e_{k3j}(\partial\phi/\partial x_k). \tag{7}$$

From Eqs. (5) and (7), the boundary conditions in Eqs. (6a)–(6d) lead to eight algebraic equations for the coefficients C_n,

$$[L]_{8\times 8}\begin{pmatrix} C_1 \\ C_2 \\ \vdots \\ C_8 \end{pmatrix}=0, \tag{8}$$

where L is a 8×8 matrix with its elements given by

$$L(n,m)=[c_{44}b^{(m)}\alpha_2^{(m)}]\exp\left[(-i)^{n-1}kb^{(m)}\frac{d}{2}\right]$$
$$(n=1,2,\ m=1-8),$$

$$L(n,m)=[c_{44}b^{(m)}\alpha_1^{(m)}+c_{44}\alpha_3^{(m)}+e_{15}\alpha_4^{(m)}]$$
$$\times\exp\left[(-i)^{n-1}kb^{(m)}\frac{d}{2}\right] \quad (n=3,4,\ m=1-8),$$

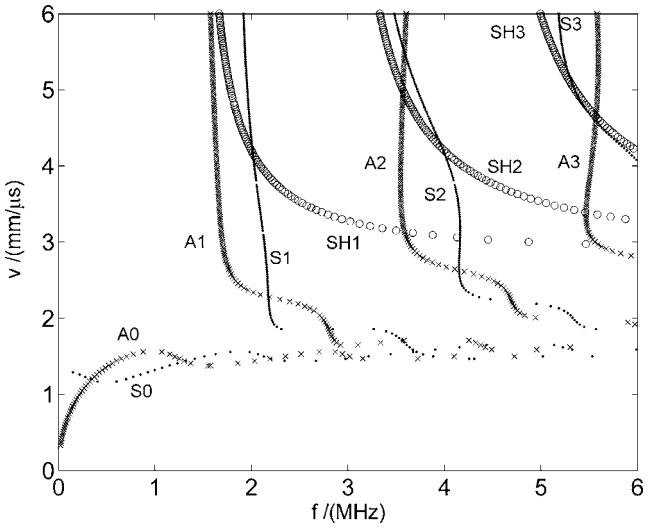

FIG. 2. Guided waves propagating along [100] of [001] poled PMN-0.33PT crystal plate for short circuit case

$$L(n,m)=[c_{13}\alpha_1^{(m)}+c_{33}b^{(m)}\alpha_3^{(m)}+e_{33}b^{(m)}\alpha_4^{(m)}]$$
$$\times\exp\left[(-i)^{n-1}kb^{(m)}\frac{d}{2}\right] \quad (n=5,6,\ m=1-8),$$

$$L(n,m)=\alpha_4^{(m)}\exp\left[(-i)^{n-1}kb^{(m)}\frac{d}{2}\right]$$
$$(n=7,8,\ m=1-8).$$

For nontrivial solutions of C_n, the determinant of the 8×8 matrix L must be zero, which gives the dispersion relation between k and v. These theoretical equations can be solved numerically to derive the dispersion relation of Lamb waves in a piezoelectric plate.

The PMN-0.33PT crystal plate studied in this work is 1 mm thick with stress-free surfaces. The Newton-simplex's algorithm is employed to calculate the dispersion curves. The results of guided waves propagating along [100] of [001] poled PMN-0.33PT crystal plate for short circuit case are shown in Fig. 2. It is found that the symmetric (S_i) and antisymmetric (A_i) modes exhibit multiple crossings as they approach the surface wave limits. Similar intercrossing dispersion relations were also found in nickel plates with free boundary conditions and a strongly orthotropic copper polycrystal plate.[10,16]

It is also noticed that as frequency increases, the velocities of the SH modes approach the bulk transversal wave velocity of 2.88 mm/μs which is coincident with the shear wave velocity in the [100] direction with displacement perpendicular to the poling direction.[15] The dispersion relations of Lamb waves propagate along [110] of [001] poled PMN-0.33PT crystal plate is shown in Fig. 3. In this direction, its Rayleigh wave velocity is about two times of that in the [100] direction, and the SH modes approach 0.88 mm/μs at high frequencies, which corresponds to the soft shear mode of bulk crystal observed in the [110] direction with displacement in the $[1\bar{1}0]$ direction.[15]

In summary, the dispersion relations of Lamb waves and SH waves propagating along the [100] and [110] directions of $[001]_c$-direction poled PMN-0.33PT single crystal plate have been calculated. These dispersion curves show multiple

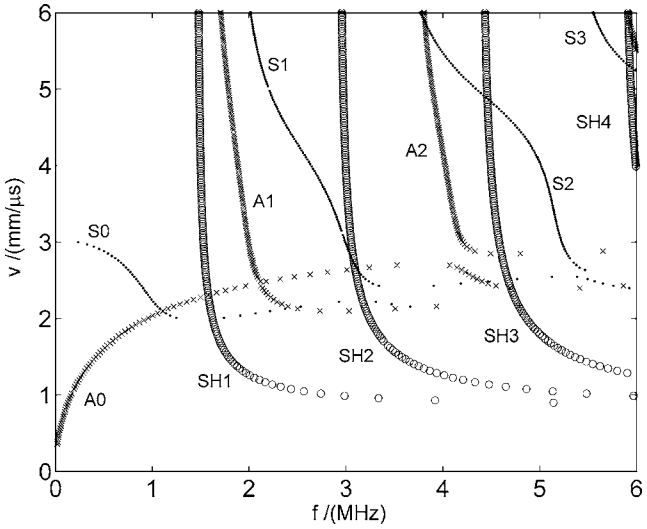

FIG. 3. Guided waves propagating along [110] of [001] poled PMN-0.33PT crystal plate for short circuit case

crossings between their symmetric and antisymmetric modes, which may due to the moderate anisotropy of the crystal. The SH modes are not coupled with the Lamb wave modes. When waves propagate along the [100] direction, the SH modes have a limit velocity of 2.88 mm/μs at very high frequencies. When guided waves propagate along the [110] direction, the SH modes have a small limiting velocity of 0.88 mm/μs, which corresponds to a soft shear mode of bulk crystal observed in the [110] direction with the displacement in the $[1\bar{1}0]$ direction.

This research is supported in part by the NSFC Under Grant No. 50602009, Program of the Ministry of Education of China for New Century Excellent Talents in University, and by the NIH under Grant No. P41-EB21820.

[1] S. E. Park and T. R. Shrout, J. Appl. Phys. **82**, 1804 (1997).
[2] Z. Yin, H. Luo, P. Wang, and G. Xu, Ferroelectrics **229**, 207 (1999).
[3] H. Luo, G. Xu, P. Wang, and Z. Yin, Ferroelectrics **231**, 97 (1999).
[4] M. Dong and Z. G. Ye, J. Cryst. Growth **209**, 81 (2000).
[5] J. Wu and Z. Zhu, IEEE Trans. Ultrason. Ferroelectr. Freq. Control **43**, 71 (1996).
[6] J. C. Andle, J. T. Weaver, J. F. Vetelino, and D. J. McAllister, Sens. Actuators B **24**, 129 (1995).
[7] M. S. Weinberg, C. E. Dube, A. Petrovich, and A. M. Zapata, J. Microelectromech. Syst. **12**, 567 (2003).
[8] Z. G. Nikiforenki, V. T. Bobrov, and I. I. Averbukh, Sov. J. Nondestruct. Test. **8**, 543 (1972).
[9] L. P. Solie and B. A. Auld, J. Acoust. Soc. Am. **54**, 50 (1973).
[10] A. H. Nayfeh and D. E. Chimenti, Trans. ASME **56**, 881 (1989).
[11] A. H. Nayfeh and H. T. Chien, J. Acoust. Soc. Am. **91**, 1250 (1992).
[12] C. H. Yang and D. E. Chimenti, Appl. Phys. Lett. **63**, 1328 (1993).
[13] C. H. Yang and D. E. Chimenti, J. Acoust. Soc. Am. **97**, 2103 (1995).
[14] S. E. Park and T. R. Shrout, IEEE Trans. Ultrason. Ferroelectr. Freq. Control **44**, 1140 (1997).
[15] R. Zhang, B. Jiang, and W. Cao, J. Appl. Phys. **90**, 3471 (2001).
[16] Y. Li and R. B. Thompson, J. Acoust. Soc. Am. **87**, 1911 (1990).